Multiple origins of cephalic sutures in trilobites and their relatives

Kun-sheng Du [a,b,1], Jin Guo [b,c,1], Sarah R. Losso [d ✉], Stephen Pates [e,✉], Ming Li [f] and Ai-lin Chen [a,g,✉]

[a] Research Center of Paleobiology, Yuxi Normal University, Yuxi 653100, China.

[b] Key Laboratory for Palaeobiology and MEC International Joint Laboratory for Palaeoenvironment, Institute of Palaeontology, Yunnan University, Kunming 650091, China.

[c] Management Committee of the Chengjiang Fossil Site World Heritage, Chengjiang, China.

[d] Museum of Comparative Zoology and Department of Organismic and Evolutionary Biology, Harvard University, Cambridge, Massachusetts 02138, USA

[e] Department of Zoology, University of Cambridge, Downing Street, Cambridge, CB2 3EJ, UK

[f] Institute of Geology, Chinese Academy of Geological Sciences, Beijing 100037, China.

[g] State Key Laboratory of Palaeobiology and Stratigraphy, Nanjing Institute of Geology and Paleontology, CAS, Nanjing, 210008, China.

✉e-mail: ailinchen@yxnu.edu.cn (A.L.C.), sarahlosso@g.harvard.edu (S.R.L.) or sp587@cam.ac.uk (S.P.).

[1] Joint first authors.

Keywords: Cambrian; arthropod; Chengjiang Biota; ecdysis; dorsal suture

Abstract

Euarthropods are an extremely diverse phylum in the modern, and have been since their origination in the early Palaeozoic. They grow through moulting the exoskeleton (ecdysis) facilitated by breaking along lines of weakness (sutures). Artiopodans, a group that includes trilobites and their non-biomineralizing relatives, dominated arthropod diversity in benthic communities during the Palaeozoic. Most trilobites – a hyperdiverse group of tens of thousands of species - moult by breaking the exoskeleton along cephalic sutures, a strategy that has contributed to their high diversity during the Palaeozoic. However, the recent description of similar sutures in early diverging non-trilobite artiopodans mean that it is unclear whether these sutures were evolved deep within Artiopoda, or evolved multiple times within the group. Here we describe new well-preserved material of *Acanthomeridion*, a putative early diverging artiopodan, including hitherto unknown details of its ventral anatomy and appendages revealed through CT scanning, highlighting additional possible homologous features between *Acanthomeridion* and trilobites. We used two coding strategies treating structures as homologous or independently derived across multiple phylogenetic analysis techniques (parsimony or Bayesian inference), and showed that regardless of these variables, the sutures crucial for the success and growth of the hyperdiverse trilobites evolved multiple times within Artiopoda.

1. Introduction

Euarthropods, more specifically members of the clade Artiopoda, dominated diversity in Palaeozoic animal communities (Daley et al., 2018). This group, which includes trilobites and their non biomineralizing relatives, are united by a morphology consisting of a headshield covering a pair of uniramous antennae and at least three pairs of biramous limbs, followed by a dorsoventrally flattened body with a series of biramous appendages (Stein and Selden, 2012; Giribet and Edgecombe, 2019). The origins of key morphological features facilitating the incredible diversity of trilobites can be found in their non-biomineralizing artiopodan relatives (Du et al., 2019; Schmidt et al., 2022). The cephalon, as an abundantly informative and functionally specialized body region, affords pivotal data for resolving the phylogenetic relationships and evolutionary history of the group (Budd and Telford, 2009; Yang et al., 2013; Strausfeld et al., 2022).

Euarthropods, as ecdysozoans (Aguinaldo et al., 1997), shed their exoskeletons to grow, a process called ecdysis (Budd and Telford, 2009; Yang et al., 2019). This process is facilitated through the presence of ecdysial sutures, which provide a line along which the exoskeleton can break, allowing the animal to escape from the old exoskeleton allowing the new cuticle to expand to a large size (Daley and Drage, 2016). The presence of dorsal cephalic sutures in trilobites – and the array of morphologies and moulting behaviours within this group – has been extensively documented (e.g. Daley and Drage 2016; Drage, 2019, 2022). The origin of dorsal cephalic sutures has traditionally been considered to fall within Trilobita. This is because olenelline trilobites, which lack dorsal sutures, are consistently resolved as the earliest diverging members of the class, making the absence of dorsal sutures appear to be a plesiomorphic character for trilobites (Lieberman, 2002). However the presence of dorsal sutures in earlier diverging artiopodans such as *Acanthomeridion* (Hou et al., 2017a; Du et al., 2019) in combination with the fusion of sutures during ontogeny for some trilobites (Drage et al., 2018), the lack of a clear link between morphology and moulting behaviour (Drage, 2022) and alternative functional demands on the location of sutures in trilobites (e.g. to facilitate burrowing, Esteve et al., 2021); have called this view into question. Alternative possibilities are that dorsal sutures had a deep root within the clade, and were subsequently lost in some artiopodans and multiple times within Trilobita, or that a facial suture was acquired independently at least twice in Artiopoda (Hou et al., 2017a; Du et al., 2019).

Resolving the phylogenetic placement of *Acanthomeridion* and other artiopodans with cephalic ecdysial sutures is crucial for resolving how many times this functionally important morphological feature evolved within the group (Hou et al., 2017a; Du et al., 2019). However, the morphology of many earlier diverging artiopodans is not completely understood (Ortega Hernández et al., 2013; Lerosey-Aubril et al., 2017), meaning that they contribute significant amounts of missing data to character matrices used in phylogenetic analyses. Up to now, *Acanthomeridion* was arguably the least well known of these early diverging artiopodans, with its ventral anatomy and soft parts very poorly known (Hou and Bergström, 1997; Hou et al., 2017a).

Here we describe new specimens of *Acanthomeridion serratum*, using micro-CT to reveal details of the ventral anatomy, eyes, and appendages for the first time, and reconstruct the changing shape of the body during ontogeny. We use these new data to show that *A. anacanthus* is a junior synonym of *A. serratum.* We then assess the phylogenetic position of the species considering two hypotheses relating to the cephalic sutures – first that they were derived independently, and second that they are homologous to the dorsal sutures of trilobites – to determine how many times these sutures evolved within Artiopoda.

2. Materials and methods

New specimens of *Acanthomeridion* were collected from Jiucun town, Chengjiang **(Fig. 1)** and accessioned at the Management Committee of the Chengjiang Fossil Site World Heritage (CJHMD 00052–00062), and Research Center of Paleobiology, Yuxi Normal University (YRCP 0016–0020). New specimens of *Wutingaspis tingi* (YRCP 0021) and *Xandarella spectaculum* (YRCP 0022) were collected from Haikou town, Kunming **(Fig. 1)** and housed at Research Center of Paleobiology, Yuxi Normal University. Holotype of *Zhiwenia coronate* (YKLP 12370) is deposited at the Key Laboratory for Palaeobiology, Yunnan University which was excavated from Xiaoshiba area, Kunming **(Fig. 1)**. The specimens were photographed by a LEICA DFC 550 digital camera mounted to a Stereoscope LEICA M205 C, and scanned with a Zeiss Xradia 520 Versa X-ray Microscope and Nikon XTH 225 ST micro-focus X-ray tomography machine. All micro-CT images were processed with the software Drishti (Zhai et al., 2019). Figures were processed with CorelDRAW X8 and Inkscape 1.0.

The character matrix used for the phylogenetic analyses was adapted from (Schmidt et al., 2022) and includes 65 taxa (*Acanthomeridion anacanthus* was removed). Two matrices were used to test the

alternative hypotheses of sutures, one with 90 characters considering the ventral plates homologous to trilobite librigenae ('ventral plates under head' as a new character in the dataset) and one with 89 characters considering them not homologous (see Morphobank project). We added the character state 'ringed distribution lamellae' to Ch. 15 in both matrices (Chen et al., 2019; Du et al., 2019; 2023). Phylogenetic analyses were performed with TNT (Maximum Parsimony) and MrBayes (Bayesian Inference) (Ronquist et al., 2012; Du et al., 2019). The parsimony analyses were run in TNT version 1.5 under New Technology Search, using Driven Search with Sectorial Search, Ratchet, Drift, and Tree fusing options activated with standard settings under equal and implied weights set to find the minimum tree length 100 times (Chen et al., 2019; Du et al., 2019). For Bayesian Inference (Ronquist et al., 2012), both the 'maximum information' and 'minimum assumptions' strategies of ref (Bapst et al., 2018) were utilised, in order to confirm that model choice was not a major driver in differences for the results. These analyses were run for 20 million generations using four chains, every 1000th sample stored and 25% burn-in (Lewis, 2001; Ronquist et al., 2012). Convergence was diagnosed using Tracer (Rambaut et al., 2018). Matrices used in phylogenetic analyses provided through morphobank (Project #P4290. Email address: P4290, reviewer password: Acanthomeridion2023).

3. Results

3.1 Systematic palaeontology

ARTIOPODA Hou and Bergström, 1997

Acanthomeridion Hou et al., 1989

Type and only species. *Acanthomeridion serratum* Hou et al., 1989

Diagnosis. Non-biomineralized artiopodan with elongate dorsal exoskeleton that gives body an elliptical outline. Subtriangular head shield with deep lateral notches that accommodate stalked elliptical eyes, rounded genal angles of the carapace, an axe-like hypostome, and paired teardrop-shaped plates on the either side of hypostome. Head bears large eyes and long multi-segmented antennae consisting of over 40 podomeres anterior to three pairs of small cephalic limbs. Trunk composed of 11 tergites bearing expanded tergopleurae with well-developed distal spines, and a terminal spine. The ninth tergite bears pleural spine more elongate than others, eleventh tergite reduced and expanded into leaf-like outline. Each tergite bears a

pair of biramous limbs with long and dense spines on the endopods, and slender stick-like exopods with long and dense bristles. Modified from Hou et al., 1989, 2017a.

Acanthomeridion serratum Hou et al., 1989

Figs. 2–5; 6g-i; S1–6

1989 *Acanthomeridion serratum* Hou et al., pl. III, figs. 1-5; pl. IV, figs. 1-5; p. 46, text-figs. 3, 4.

1996 *Acanthomeridion serratum* Chen et al., p. 157, figs 199-203.

1997 *Acanthomeridion serratum* Hou and Bergström, p. 38.

1999 *Acanthomeridion serratum* Luo et al., p. 51, pl. 6 fig. 5.

1999 *Acanthomeridion serratum* Hou et al., p. 130, fig. 188.

2004 *Acanthomeridion serratum* Chen, p. 280, fig. 442.

2004 *Acanthomeridion serratum* Hou et al., p. 176, fig. 16.63; p. 177, fig. 16.64.

2017a *Acanthomeridion serratum*, *A. anacanthus*, and *Acanthomeridion* sp in Hou et al., p. 734, figs. 1-4.

2017b *Acanthomeridion serratum* Hou et al., p. 204, fig. 20.34; p. 205, fig. 20.35.

Type material. *Holotype*, CN 108305. *Paratype*, CN 108306–108310.

New material. Sixteen new specimens were collected from Jiucun **(Fig. 1)**, Chengjiang County and housed in the Management Committee of the Chengjiang Fossil Site World Heritage (CJHMD 00052–00062), and Research Center of Paleobiology, Yuxi Normal University (YRCP 0016–0020).

Occurrence. Yu'anshan Member, Qiongzhusi Formation, *Wutingaspis–Eoredlichia* biozone, Cambrian Stage 3. Jiucun and Maotianshan, Chengjiang County, Yunnan, China; Mafang and Ercaicun, Haikou town, Kunming, Yunnan, China **(Fig. 1)**.

Diagnosis. As for genus, by monotypy.

Description. The dorsal exoskeleton of *Acanthomeridion serratum* displays weak trilobation and elliptical outline. Specimens measure from 20 to 75 mm along the sagittal axis (**Figs. 2a, c; 3a; 4; S1–6**). The head shield is subtriangular in dorsal view, with rounded anterior margin and small spines on posterior margin (**Figs. 2a, c; 3a; 4; S6a, c**). A pair of lateral posterior notches accommodate stalked elliptical eyes. The lateral margin of the head shield is a suture that attaches paired ventral plates. Ventral plates have a teardrop outline, occupy the entire length of the cephalon and terminate in a posterior spine (maximum length 3.4 mm; **Fig. S2b**) that projects into the thorax as far as the anteriormost tergite (**Fig. S1a**). The medial margin is curved towards the axially line and sits adjacent to a conterminant axe-shaped hypostome

(maximum dimensions 9.6 mm x 11.6 mm; **Fig. 2a, b**). Four pairs of appendages are present in the head (**Figs. 2f–j; S5a**). A pair of antennae with at least 43 segments (**Figs. 3a, b; S2a, f; S4b**) sit anterior to three pairs of small cephalic limbs (**Fig. 2f–j**). The cephalic appendages are poorly preserved and only the gross morphology can be discerned as no individual podomeres are visible. The protopodite of the cephalic limbs are subtriangular in outline. Endopodites and exopodites are not clearly preserved. Appendage three may include the endopodite, but no podomeres are visible.

The trunk is composed of 11 tergites which extend laterally into spinose tergopleurae. Tergites are all subequal in length. Tergites 8-11 curve towards the posterior, and reduce in width progressively, so that T11 is approximately 25% the width of T8 and 33% the width of T9 (**Figs. 2a, c; 3a; S1a, c, d**). Each tergite has small spines on its lateral and posterior margins (**Figs. 5; S1a, c–f; S2i, k; S3a, j; S5b, e, f; S6a–f**). The shape of tergites and the convexity of the trunk changes through ontogeny (**Fig. 4**). In the smaller specimens, the trunk appears slender from a dorsal view as the body displays a high convexity (**Fig. 4t**). Pleurae curve ventrally, and only slightly towards the posterior (**Fig. 4a–k**). In larger specimens, the trunk is less convex than for the smaller specimens (**Fig. 4s**), ventral curvature of pleurae is decreased, and posterior curvature increased (**Fig. 4o–r**). Where trunk appendages are preserved, each tergite is associated with a pair of biramous trunk appendages (**Figs. 2a, c, h, k; 3; S1a, b**). The protopodite is sub triangular with a broad attachment to the body wall and short studline gnathobasal spines along the medial margin (**Figs. 2h–j; S3a–f, i**). The ventral margin of the protopodite has endites longer than the gnathobasal spins. The dorsal edge of the protopodite is poorly preserved and does not clearly show the attachment of the exopodite. Exopodites are slender, stick-like and long (8.3 mm, ca. 3x protopodite length), bearing two rows of lamellae (**Figs. 2h, k; S1a, b**). Exopods are shorter than the width of corresponding tergites **(Figs. 2h, S1a, b)**. The lamellae appear short but may not be completely preserved. There is no evidence that the exopodite divided into lobes or has articulations. Endopodites are composed of seven trapezoidal podomeres. Podomeres 1–6 bear spiniferous endites arranged in rows, six on pd1, 2, four on pd3, 4, and three on pd5, 6. Podomere seven displays a terminal claw of three elongate spines (**Figs. 2h, k; 3d**). From the preserved appendages, no significant antero-posterior differentiation or dramatic size reduction can be discerned (**Figs. 2, S1**) One specimen shows evidence for paired midgut diverticulae **(Fig. S4a, f**). The body terminates in a long, slender spine, dorsal to a paired paddle-like structure (**Figs. 3a, e; S5b, g**).

Remarks. The eyes were identified as genal projections (see Fig. 1, Fig. 2A, and Fig. 3A in Hou et al., 2017a) because of the limited available specimens and the posterior location of the eyes. *Acanthomeridion anacanthus* Hou et al. 2017a is a junior subjective synonym of *Acanthomeridion serratum* Hou et al.1989 based on:

1) The paddle-like structure under the terminal spine **(Figs. 3a, e; S5b, g)** was previously interpreted as the twelfth tergite. The specimen YKLP 11115 (see Fig.4 in Hou et al., 2017a) which is a similar size to YKLP 11116 (holotype of *Acanthomeridion anacanthus*) and YKLP 11113 (see Fig.2A, C and Fig.3A, C in Hou et al., 2017a) show 11 tergites.

2) Specimens CJHMD 00052-55 and YRCP 0016 show the evidently pleural spines of T8 and T9 **(Figs. 2a, c; 3a; S1a, c, d; S2a, f; S4b, g)**.

3) The orientation of pleurae makes some specimens look like narrower than others. Specifically, those where pleurae curve ventrally look more slender than those where pleurae are curved posteriorly. Specimen YRCP 0017 preserves right ventrally curving pleura and left flat pleura, which lead to its right pleura narrower than the left **(Figs. 4j, o; S2i)**. Moreover, most small specimens (1cm–3cm) are preserved with ventrally curving pleurae **(Figs. 4a–e; S3a–c; S4a; S5a-c; S6g, i)** and these appear narrower than the few small specimens with flat pleurae (**Figs. 4f; S4b**. See also Fig.2A–D, and Fig.4 in Hou et al., 2017a). Larger specimens are typically preserved with flattened, posteriorly curving pleurae.

4) The sixteen new specimens with different size show a good ontogenetic series of *Acanthomeridion* including some that would previously have been assigned to '*Acanthomeridion anacanthus*' in the absence of data preserving the whole series **(Fig. 4)**.

The new specimens and CT data presented herein allow the description of cephalic and trunk limbs, and a conterminant hypostome adjacent to ventral plates in *Acanthomeridion* for the first time. The librigena-like ventral plates bearing a terminal spine and attaching head with dorsal sutures are like the librigenae of opisthoparian trilobites **(Fig. 6a, b)** (Whittington et al., 1997). The dorsal suture is an oblique line that passes near its compound eye, which is extremely similar the facial suture of trilobites especially these bearing opisthoparian facial sutures **(Fig. 6a, b)** (Whittington et al., 1997), moreover, it is also like that of *Xandarella* **(Fig. 6c, d)** (Hou and Bergström, 1997) and *Phytophitaspis* (Ivantsov, 1999), and the notches of *Luohuilinella* and *Zhiwenia* **(Fig. 6e, f)** which were interpreted as dorsal ecdysial sutures owing

to their close morphological and positional similarities (Zhang et al., 2012; Du et al., 2019; Hou et al., 2019). The presence of four appendages in the head (or three in the head and one underneath the articulation) is comparable to *Zhiwenia* (Du et al., 2019), as well as other artiopodans including trilobites (Edgecombe and Ramsköld, 1999). However, the morphology of the three non-antenniform cephalic limbs is difficult to determine with only the protopodite clearly visible. The lack of observed endopodites and exopodites on these three appendages may be a preservational artefact. Possibly the absence of clear endopodites and exopodites represents specialization of the cephalic appendages with the structures being significantly reduced. Other Cambrian artiopodans have been shown to have appendage specialization (Losso and Ortega-Hernández, 2022) which is frequently found in the cephalon (Chen et al., 2019; Schmidt et al., 2022), but none show reduction of both the exopodite or endopodite. In *Sinoburius lunaris*, the first two post-antennal appendages have reduced endopodites with elongated exopodites (Chen et al., 2019), and in *Pygmaclypeatus daziensis* the exopodite is significantly reduced in the cephalic appendages (Schmidt et al., 2022). Recently, the head of *Retifacies abnormalis* was interpreted to develop three pairs of uniramous post-antennal appendages and following by one biramous appendage pair (Zhang et al., 2022). It would be unclear the function of an appendage with both distal elements being significantly reduced until more clear appendages are found.

The exopodites of *Acanthomeridion* also differ substantially from those known in other artiopodans. Specifically, the stick like nature of the exopodite, the rows of lamellae combined with the apparent lack of segmentation, differ from the paddle shaped exopodites thought to characterise the remainder of the group (e.g. Schmidt et al., 2022, Du et al., 2023, and fig. 4 in Ortega Hernández et al., 2013).

3.2 Phylogenetic analyses

In order to test how many times ecdysial sutures evolved within Artiopoda, we used two distinct coding strategies in our phylogenetic analyses (**Figs. 7; S7–9)**. Firstly, we considered the cephalic sutures of *Acanthomeridion* and *Zhiwenia* and the presence of eye slits in petalopleurans, as distinct from the ecdysial

sutures in trilobites. In a second set of analyses we treated all these features as homologous, and the terminal spine on the ventral plate of *Acanthomeridion* as homologous to the genal spine of trilobites.

Consensus trees of analyses using the first coding strategy (sutures not homologous) broadly resemble other recent studies, with Vicissicaudata, Nektaspida, Petalopleura, Conciliterga and Trilobita recovered as monophyletic groups (with the latter four recovered in a monophyletic Trilobitomorpha for the parsimony analyses) (**Figs. 7a, b; S7a)**. *Acanthomeridion* was not recovered within Protosutura in any consensus tree, though in the parsimony analyses *Zhiwenia* and *Australimicola* (the other members of Protosutura) were recovered as sister taxa. *Acanthomeridion* was instead recovered as an early diverging member of Artiopoda (in a polytomy with *Kwanyinaspis maotiashanensis* and three clades in the parsimony analyses, or in a more poorly resolved polytomy for the Bayesian analyses) (**Figs. 7a, b; S7a; S8a; S9a)**.

Consensus trees of analyses using the second coding strategy (sutures coded as homologous) recovered *Acanthomeridion* as sister to trilobites (here represented by *Eoredlichia intermedia* and *Olenoides serratus*), with the exception of the 'minimum assumptions' consensus, where *Acanthomeridion* was instead recovered in a polytomy with eight other taxa and five clades (**Figs. 7c, d; S7b; S8b)**. Both Bayesian and parsimony analyses recovered *Australimicola* as sister to Conciliterga, while the parsimony analysis resolved *Zhiwenia* as sister to Petalopleura (**Figs. 7c, d; S7b; S8b)**. The Bayesian consensus trees recovered monophyletic Nektaspida, Petalopleura, Conciliterga and Trilobita and a polyphyletic Vicissicaudata, though the relationships between these groups were not resolved, with the exception of Petalopleura + Nektaspida (**Figs. 7d; S7b; S8b)**. The parsimony consensus trees recovered well resolved relationships between the major constituent groups of artiopodan, albeit one very different to other recent studies (**Figs. 7c; S7b)**. Petalopleura (+ *Zhiwenia*) represents the earliest diverging group of artiopodans in these results. Nektaspida, Trilobita (+ *Retifacies* + *Acanthomeridion*), *Bailongia* form a paraphyletic assemblage, leading to Conciliterga (+*Kwanyinaspis, Australimicola*) and Vicissicaudata as the last diverging groups (**Figs. 7c; S7b)**.

4. Discussion and conclusion

All consensus trees, of parsimony and Bayesian results from both coding strategies, support multiple origins of cephalic sutures in Artiopoda (**Fig. 7**). Analyses coding the sutures of trilobites as distinct from comparable cephalic features in *Acanthomeridion, Zhiwenia* and petalopleurans recover topologies similar to other recent studies. However, *Acanthomeridion* is not recovered within Protosutura. Instead, there is a polytomy at the base of Artiopoda including these taxa, Trilobitomorpha and Vicissicaudata (or, in the Bayesian consensus trees, a more poorly resolved polytomy). These results support at least three independent origins of cephalic sutures in artiopodans – once within trilobites, a second time in petalopleurans, and a third time in protosuturans, with the unresolved position of *Acanthomeridion* offering a possible fourth origin. Results of analyses where cephalic sutures in *Acanthomeridion, Zhiwenia* and petalopleurans are considered homologous to those in trilobites, recover *Acanthomeridion* as sister to Trilobita. Despite the differences in the topologies of parsimony and Bayesian analyses, a deep origin for cephalic sutures in Artiopoda is not well supported, and nor are all taxa coded as possessing sutures recovered together. The results support two separate origins for cephalic sutures (*Zhiwenia* + Petalopleura and *Acanthomeridion* + Trilobita), as this represents a more parsimonious scenario than the alternative - a single origin at the base of Artiopoda and at least four losses (*Squamacula, Nektaspida, Retifacies, Bailongia* + Conciliterga + Vicissicaudata). Under this coding strategy, Protosutura is not recovered. Instead, *Australimicola* is resolved as sister to concilitergans, while *Zhiwenia* is found sister to petalopleurans (parsimony) or not well resolved (Bayesian).

Other features observed in *Acanthomeridion* for the first time – uniramous deutocererbral appendages, an axe-shaped conterminant hypostome, two librigenal-like plates and three additional head appendages – are consistent with a phylogenetic position for the species as an early diverging artiopodan, or as sister to trilobites. Multipodomerous uniramous deutocerebral antennae are known in nearly all other members of the clade (Zhang et al., 2007; Du et al., 2019; Zhai et al., 2019), and thus this feature is not very informative. Similarly, a conterminant hypostome was already known in numerous other artiopodans

(Zhang et al., 2004; Stein and Selden, 2012). As this type of hypostomal attachment is considered ancestral within Trilobita (Fortey, 1990), its presence in the possible sister to trilobites (if cephalic sutures are considered homologous) does not have broad evolutionary implications. If *Acanthomeridion* is instead an

early diverging artiopodan, the presence of natant hypostomes in both trilobitomorphs and vicissicaudates (Fortey, 1990; Chen et al., 2019) demonstrates that a natant hypostome has most likely evolved repeatedly within Artiopoda. The ventral plate of *Acanthomeridion* is very similar to the free cheek of trilobites developing opisthoparian facial sutures (e.g. Redlichiina) by termination with a spine and attaching head with dorsal suture which is an oblique line and passes near the eye both for *Acanthomeridion* and trilobites bearing opisthoparian facial sutures (Whittington et al., 1997). Together with trilobate exoskeleton of large specimens, and endopods bearing seven podomeres, the non biomineralised *Acanthomeridion* bears may morphological similarities to biomineralised trilobites.

Acanthomeridion displays an unusual organisation of the head region, where the axe-shaped hypostome and two librigena-like plates appear to cover the entire ventral surface. The reduced post-antennal cephalic appendages combined with the hypostome and librigenal like plates were likely specialized for feeding. Such ventral head structures are unknown from other fossil arthropods, or even extant arthropods (Edgecombe, 2020), e.g. radiodonts (Potin and Daley 2023), fuxianhuiids (Yang et al., 2018), Cambrian bivalved arthropods (Zhang et al., 2023), megacheirans (Liu et al., 2020), artiopodans excluding *Acanthomeridion* (Ortega Hernández et al., 2013; Jiao et al., 2022), chelicerates and mandibulates (Brusca et al., 2016). One ecological interpretation is that *Acanthomeridion* may have used its head to plough through the sediment, using endopodites bearing long endites to catch food items, while the large ventral plates and hypostome protected the non-biomineralized structures and directed sediment.

In summary, new fossils and CT-scan data reveals the ventral anatomy and appendages of *Acanthomeridion serratum* for the first time, and additional specimens demonstrate that *A. 'anacanthus'* represents a junior synonym of *A. serratum,* with some features thought to distinguish the two instead ontogenetic in origin. The presence of a posteriorly orientated spine on the cephalic ventral plates of *Acanthomeridion* might be homologous to the genal spine of trilobite librigenae, providing support for treating the ventral plates of *A. serratum* as homologous to these free cheeks. However, regardless of the coding strategy concerning the nature of cephalic sutures in *Acanthomeridion, Zhiwenia* and petalopleurans (homologous to those of trilobites or not), and the resulting position of *Acanthomeridion* within Artiopoda, all results support multiple origins of cephalic sutures in the group rather than a single, deep origin.

Conflict of interest

The authors declare that they have no conflict of interest.

Acknowledgments

We thank Jian Han and Jie Sun for scanning the fossils and Javier Ortega-Hernández for helpful discussion. This work was supported by the National Natural Science Foundation of China (grant numbers 42262004, 42202003, 41662003), State Key Laboratory of Palaeobiology and Stratigraphy (Nanjing Institute of Geology and Palaeontology, CAS) (No. 193104). Stephen Pates acknowledges support from a Herchel Smith Postdoctoral Fellowship (University of Cambridge).

CRediT authorship contribution statement

Kunsheng Du: Conceptualization, Data Curation, Investigation, Formal analysis, Methodology, Visualization, Writing – original draft, Writing – review and editing, Supervision. **Jin Guo:** Resources, Data curation, Validation. **Sarah R. Losso:** Conceptualization, Data Curation, Formal analysis, Writing – original draft, Writing – review and editing. **Stephen Pates:** Conceptualization, Data Curation, Investigation, Formal analysis, Methodology, Visualization, Writing – original draft, Writing – review and editing, Supervision. **Ming Li:** Methodology, Data curation. **Ailin Chen:** Resources, Funding acquisition, Project administration, Visualization, Validation, Writing – review and editing, Supervision.

References

Aguinaldo, A.M.A., Turbeville, J.M., Linford, L.S., Rivera, M.C., Garey, J.R., Raff, R.A., Lake, J.A., 1997. Evidence for a clade of nematodes, arthropods and other moulting animals. Nature. 387, 489-493.

Bapst, D.W., Schreiber, H.A., Carlson, S.J., 2018. Combined analysis of extant Rhynchonellida (Brachiopoda) using morphological and molecular data. Syst. Biol. 67, 32-48.

Brusca, R.C., Moore, W., Shuster, S.M., 2016. Invertebrates, Third 3rd Edition. Sinauer Associates Inc., Sunderland, Massachusetts U.S.A, 711-961 pp.

Budd, G.E., Telford, M.J., 2009. The origin and evolution of arthropods. Nature. 457, 812-817.

Chen, J.Y., 2004. The dawn of animal world. Jiangsu Science and Technology Publishing House, Nanjing, 365 pp [in Chinese].

Chen, J.Y., Zhou, G.Q., Zhu, M.Y., Yeh, K.Y., 1996. The Chengjiang biota: a unique window of the Cambrian explosion, Taichung, Taiwan, 222 pp [in Chinese].

Chen, X.H., Ortega-Hernández, J., Wolfe, J.M., Zhai, D.Y., Hou, X.G., Chen, A.L., Mai, H.J., Liu, Y., 2019. The appendicular morphology of *Sinoburius lunaris* and the evolution of the artiopodan clade Xandarellida (Euarthropoda, early Cambrian) from South China. BMC Evol. Biol. 19, 165.

Daley, A.C., Antcliffe, J.B., Drage, H.B., Pates, S., 2018. Early fossil record of Euarthropoda and the Cambrian Explosion. Proc. Natl. Acad. Sci. USA. 115, 5323-5331.

Daley, A.C., Drage, H.B., 2016. The fossil record of ecdysis, and trends in the moulting behaviour of trilobites. Arthropod Struct. Dev. 45, 71-96.

Drage, H.B., 2019. Quantifying intra-and interspecific variability in trilobite moulting behaviour across the Palaeozoic. Palaeontol. Electron. 22, 1-39. https://doi.org/10.26879/940

Drage, H.B., 2022. Trilobite moulting behaviour variability had little association with morphometry. bioRxiv. https://doi.org/10.1101/2022.12.12.520015

Drage, H.B., Laibl, L., Budil, P., 2018. Postembryonic development of Dalmanitina, and the evolution of facial suture fusion in Phacopina. Paleobiology. 44, 638-659.

Du, K.S., Bruton, D.L., Yang, J., Zhang, X.G., 2023. An early Cambrian *Sidneyia* (Arthropoda) resolves the century-long debate of its head organization. Sci. China Earth Sci. 66, 521-527.

Du, K.S., Ortega Hernández, J., Yang, J., Zhang, X.G., 2019. A soft-bodied euarthropod from the early Cambrian Xiaoshiba Lagerstätte of China supports a new clade of basal artiopodans with dorsal ecdysial sutures. Cladistics. 35, 269-281.

Edgecombe, G.D., 2020. Arthropod origins: integrating paleontological and molecular evidence. Annu. Rev. Ecol. Evol. Syst. 51, 1-25.

Edgecombe, G.D., Ramsköld, L., 1999. Relationships of Cambrian Arachnata and the systematic position of Trilobita. J. Paleontol. 73, 263-287.

Esteve, J., Marcé Nogué, J., Pérez Peris, F., Rayfield, E., 2021. Cephalic biomechanics underpins the evolutionary success of trilobites. Palaeontology. 64, 519-530.

Fortey, R.A., 1990. Ontogeny, hypostome attachment and trilobite classification. Palaeontology. 33, 529-576.

Giribet, G., Edgecombe, G.D., 2019. The Phylogeny and Evolutionary History of Arthropods. Curr. Biol. 29, R592-R602.

Hou, X.G., Aldridge, R.J., Bergström, J., Siveter, D.J., Siveter, D.J., Feng, X.H., 2004. The Cambrian fossils of Chengjiang, China: the flowering of early animal life, 233. Wiley Online Library, Oxford, 233 pp.

Hou, X.G., Bergström, J., 1997. Arthropods of the Lower Cambrian Chengjiang fauna, southwest China. Foss. Strat. 45, 1-116.

Hou, X.G., Bergström, J., Feng, X.H., Wang, H.F., Chen, A.L., 1999. The Chengjiang Fauna: exceptionally well-preserved animals from 530 million years ago. Yunnan Science and Technology Press, Kunming, 170 pp [in Chinese with English summary].

Hou, X.G., Chen, J.Y., Lu, H.Z., 1989. Early Cambrian new arthropods from Chengjiang, Yunnan. Acta Palaeontol. Sin. 28, 42-57.

Hou, X.G., Siveter, D.J., Siveter, D.J., Aldridge, R.J., Cong, P.Y., Gabbott, S.E., Ma, X.Y., Purnell, M.A., Williams, M., 2017b. The Cambrian fossils of Chengjiang, China: The flowering of early animal life. John Wiley & Sons, Oxford.

Hou, X.G., Williams, M., Gabbott, S., Siveter, D.J., Siveter, D.J., Cong, P.Y., Ma, X.Y., Sansom, R., 2017a. A new species of the artiopodan arthropod *Acanthomeridion* from the lower Cambrian Chengjiang Lagerstätte, China, and the phylogenetic significance of the genus. J. Syst. Palaeontol. 15, 733-740.

Hou, X.G., Williams, M., Sansom, R., Siveter, D.J., Siveter, D.J., Gabbott, S., Harvey, T.H.P., Cong, P.Y., Liu, Y., 2019. A new xandarellid euarthropod from the Cambrian Chengjiang biota, Yunnan Province, China. Geol. Mag. 156, 1375-1384.

Ivantsov, A.Y., 1999. Trilobite-like arthropod from the Lower Cambrian of the Siberian Platform. Acta Palaeontol. Pol. 44, 455-466.

Jiao, D.G., Du, K.S., Zhang, X.G., Yang, J., Eggink, D., 2022. A new small soft-bodied non-trilobite artiopod

from the Cambrian Stage 4 Guanshan Biota. Geol. Mag. 159, 730-734.

Lerosey-Aubril, R., Zhu, X.J., Ortega-Hernández, J., 2017. The Vicissicaudata revisited-insights from a new aglaspidid arthropod with caudal appendages from the Furongian of China. Sci. Rep. 7, 1-18.

Lewis, P.O., 2001. A likelihood approach to estimating phylogeny from discrete morphological character data. Syst. Biol. 50, 913-925.

Lieberman, B.S., 2002. Phylogenetic analysis of some basal early Cambrian trilobites, the biogeographic origins of the Eutrilobita, and the timing of the Cambrian radiation. J. Paleontol. 76, 692-708.

Liu, Y., Ortega-Hernández, J., Zhai, D.Y., Hou, X.G., 2020. A reduced labrum in a Cambrian great-appendage euarthropod. Curr. Biol. 30, 3057-3061.

Losso, S.R., Ortega-Hernández, J., 2022. Claspers in the mid-Cambrian *Olenoides serratus* indicate horseshoe crab‐like mating in trilobites. Geology. 50, 897-901.

Luo, H.L., Hu, S.X., Chen, L.Z., Zhang, S.S., Tao, Y.H., 1999. Early Cambrian Chengjiang Fauna From Kunming Region China. Yunnan Science and Technology Press, Kunming, 181 pp [in Chinese with English summary].

Ortega Hernández, J., Legg, D.A., Braddy, S.J., 2013. The phylogeny of aglaspidid arthropods and the internal relationships within Artiopoda. Cladistics. 29, 15-45.

Potin, G. J. M., Daley, A. C. (2023). The significance of *Anomalocaris* and other Radiodonta for understanding paleoecology and evolution during the Cambrian explosion. Front. Earth. Sci. 11, 591. https://doi.org/10.3389/feart.2023.1160285

Rambaut, A., Drummond, A.J., Xie, D., Baele, G., Suchard, M.A., 2018. Posterior summarization in Bayesian phylogenetics using Tracer 1.7. Syst. Biol. 67, 901-904.

Ronquist, F., Teslenko, M., Van Der Mark, P., Ayres, D.L., Darling, A., Höhna, S., Larget, B., Liu, L., Suchard, M.A., Huelsenbeck, J.P., 2012. MrBayes 3.2: efficient Bayesian phylogenetic inference and model choice across a large model space. Syst. Biol. 61, 539-542.

Schmidt, M., Hou, X.G., Zhai, D.Y., Mai, H.J., Belojevi, J., Chen, X.H., Melzer, R.R., Ortega-Hernández, J., Liu, Y., 2022. Before trilobite legs: *Pygmaclypeatus daziensis* reconsidered and the ancestral appendicular organization of Cambrian artiopods. Philos. T. R. Soc. B. 377. https://doi.org/10.1098/rstb.2021.0030

Stein, M., Selden, P.A., 2012. A restudy of the Burgess Shale (Cambrian) arthropod *Emeraldella brocki* and reassessment of its affinities. J. Syst. Palaeontol. 10, 361-383.

Strausfeld, N.J., Hou, X., Sayre, M.E., Hirth, F., 2022. The lower Cambrian lobopodian Cardiodictyon resolves

the origin of euarthropod brains. Science. 378, 905-909.

Whittington, H.B., Chatterton, B., Speyer, S.E., Fortey, R.A., Owens, R.M., Chang, W.T., Dean, W.T., Jell, P.A., Laurie, J.R., Palmer, A.R., 1997. Treatise on Invertebrate Paleontology, Part O, Arthropoda 1, Trilobita, Revised, pp. 530.

Yang, J., Ortega-Hernández, J., Butterfield, N.J., Zhang, X.G., 2013. Specialized appendages in fuxianhuiids and the head organization of early euarthropods. Nature. 494, 468-471.

Yang, J., Ortega-Hernández, J., Drage, H.B., Du, K.S., Zhang, X.G., 2019. Ecdysis in a stem-group euarthropod from the early Cambrian of China. Sci. Rep. 9. https://doi.org/10.1038/s41598-019-41911-w

Yang, J., Ortega-Hernández, J., Legg, D.A., Lan, T., Hou, J.B., Zhang, X.G., 2018. Early Cambrian fuxianhuiids from China reveal origin of the gnathobasic protopodite in euarthropods. Nat. Commun. 9. https://doi.org/10.1038/s41467-017-02754-z

Zhai, D.Y., Edgecombe, G.D., Bond, A.D., Mai, H.J., Liu, Y., 2019. Fine-scale appendage structure of the Cambrian trilobitomorph *Naraoia spinosa* and its ontogenetic and ecological implications. P. Roy. Soc. B-Biol. Sci. 286, 20192371. https://doi.org/10.1098/rspb.2019.2371

Zhang, C.X., Liu, Y., Ortega-Hernández, J., Wolfe, J.M., Jin, C.F., Mai, H.J., Hou, X.G., Guo, J., Zhai, D.Y., 2023. Three-dimensional morphology of the biramous appendages in *Isoxys* from the early Cambrian of South China, and its implications for early euarthropod evolution. P. Roy. Soc. B-Biol. Sci. 290, 20230335. https://doi.org/10.1098/rspb.2023.0335

Zhang, M.Y., Liu, Y., Hou, X.G., Ortega-Hernández, J., Mai, H.J., Schmidt, M., Melzer, R.R., Guo, J., 2022. Ventral Morphology of the Non-Trilobite Artiopod *Retifacies abnormalis* Hou, Chen & Lu, 1989, from the Early Cambrian Chengjiang Biota, China. Biology. 11, 1235. https://doi.org/10.3390/biology11081235

Zhang, X.L., Fu, D.J., Dai, T., 2012. A new xandarellid arthropod from the Chengjiang Lagerstätte, Lower Cambrian of Southwest China. Geobios. 45, 335-338.

Zhang, X.L., Han, J., Zhang, Z.F., Liu, H.Q., Shu, D.G., 2004. Redescription of the Chengjiang arthropod *Squamacula clypeata* Hou and Bergström, from the Lower Cambrian, south-west China. Palaeontology. 47, 605-617.

Zhang, X.L., Shu, D.G., Erwin, D.H., 2007. Cambrian naraoiids (Arthropoda): morphology, ontogeny, systematics, and evolutionary relationships. J. Paleontol. 81, 1-52.

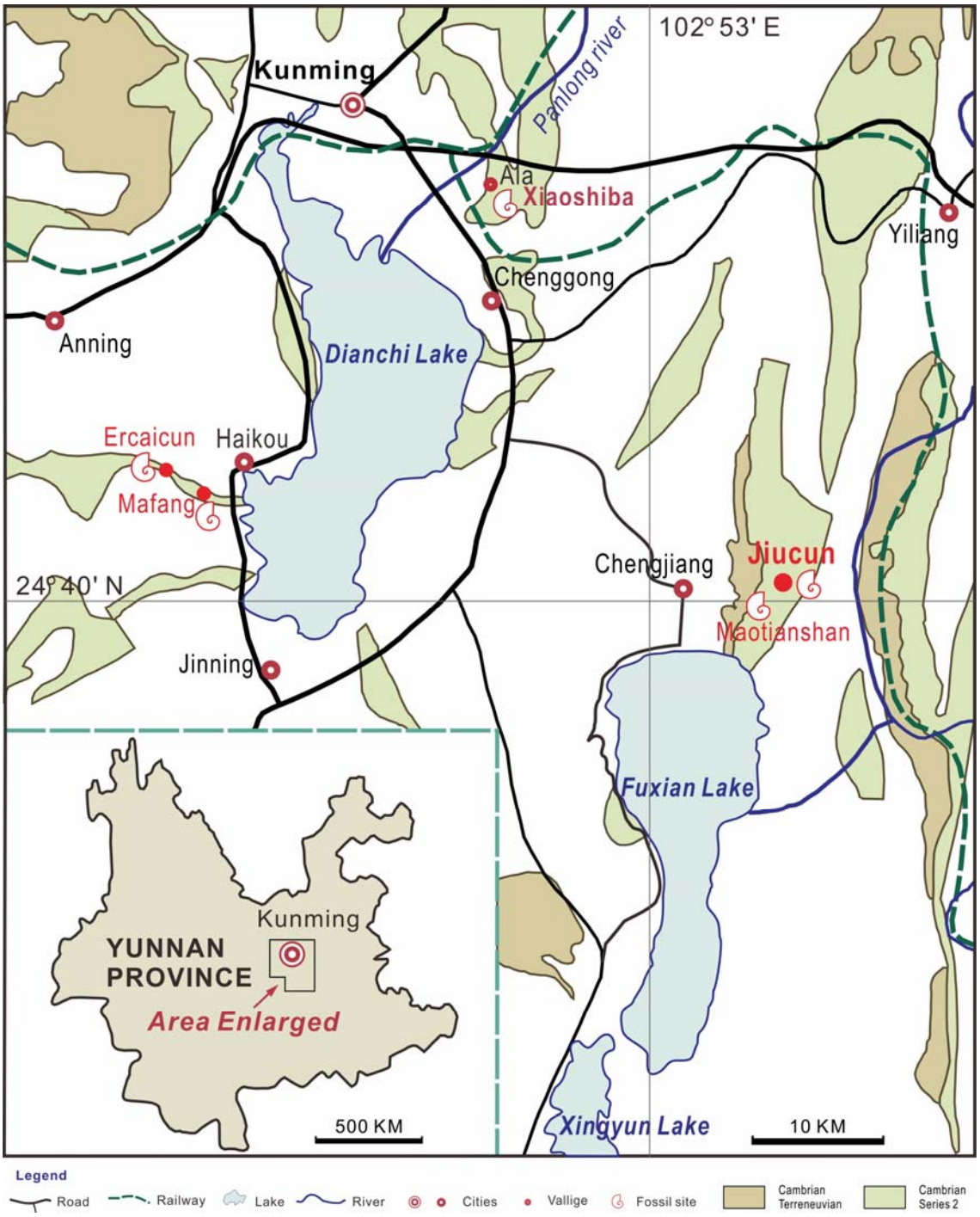

Fig. 1 Sites yielding *Acanthomeridion* from the Cambrian Stage 3 Chengjiang Biota (red circles). All the specimens of *A. serratum* used here are collected from Jiucun town, Chengjiang County.

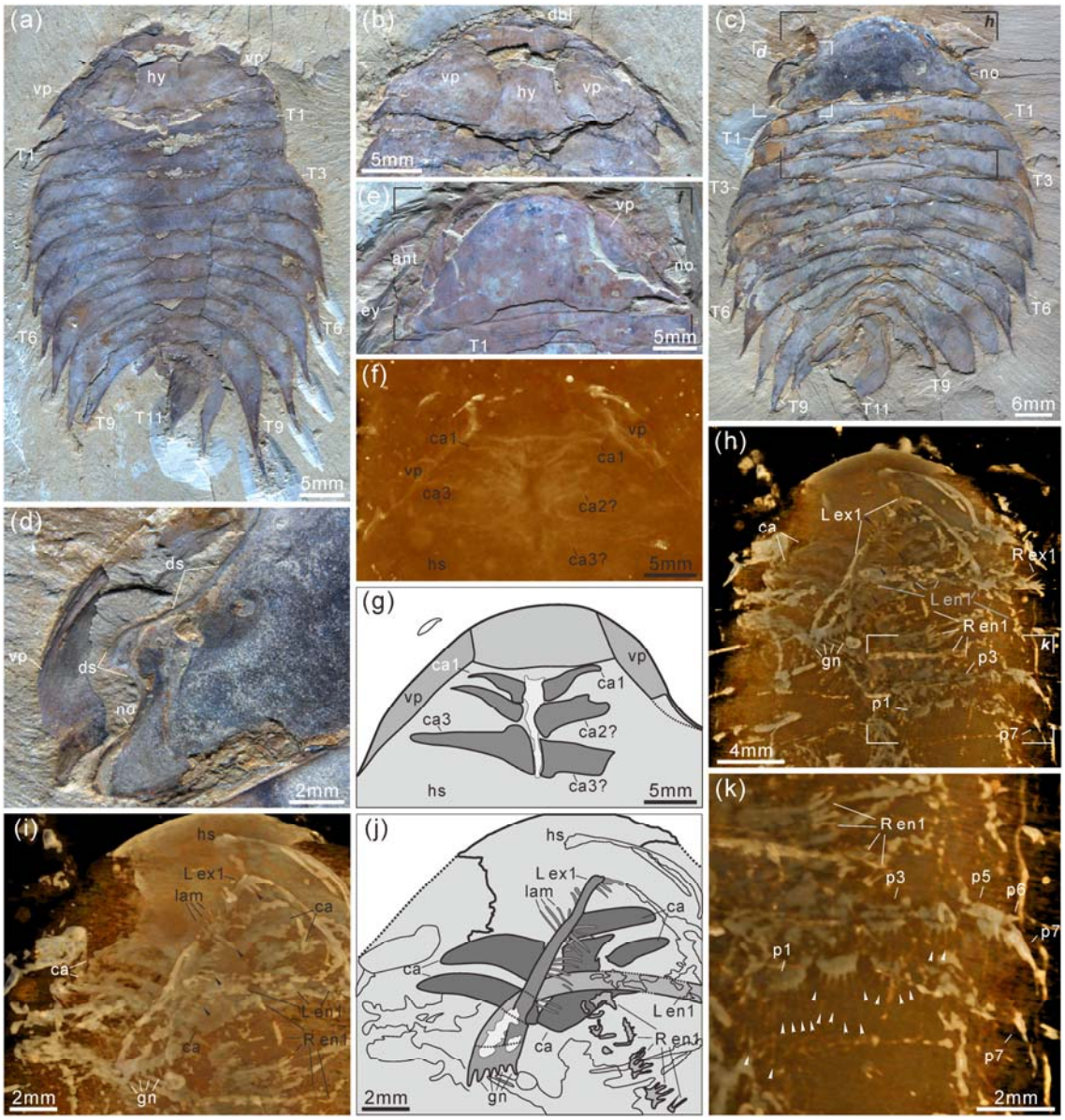

Fig. 2 *Acanthomeridion serratum* from the Cambrian Stage 3 Chengjiang Biota. (a, b) CJHMD 00052a/b respectively, individual with hypostome, ventral plates, and 11 tergites. (c, d) CJHMD 00053a, showing ventral plate, dorsal sutures, and 11 tergites. (e–g) YRCP 0016a, showing the ventral plates, and three post-antennal limbs. (h–k) Showing the post-antennal appendages under head, gnathobases of trunk limbs, stick-like exopodites with bristles (black arrows), and endopodites with long spines (white arrows). (f) Micro-CT image of YRCP 0016a; (h, i, k) Micro-CT images of CJHMD 00053a. Abbreviations: ant, antenna; ca*n*, post-antennal appendage *n* beneath head; dbl, doublure; ds, dorsal suture; en, endopodites; ex, exopodites; ey, eye; hs, head shield; hy, hypostome; L, left; lam, lamellae; no, notch; p*n*, podomere *n*; R, right; T*n*, tergite *n*; ts, terminal spine; vp, ventral plate.

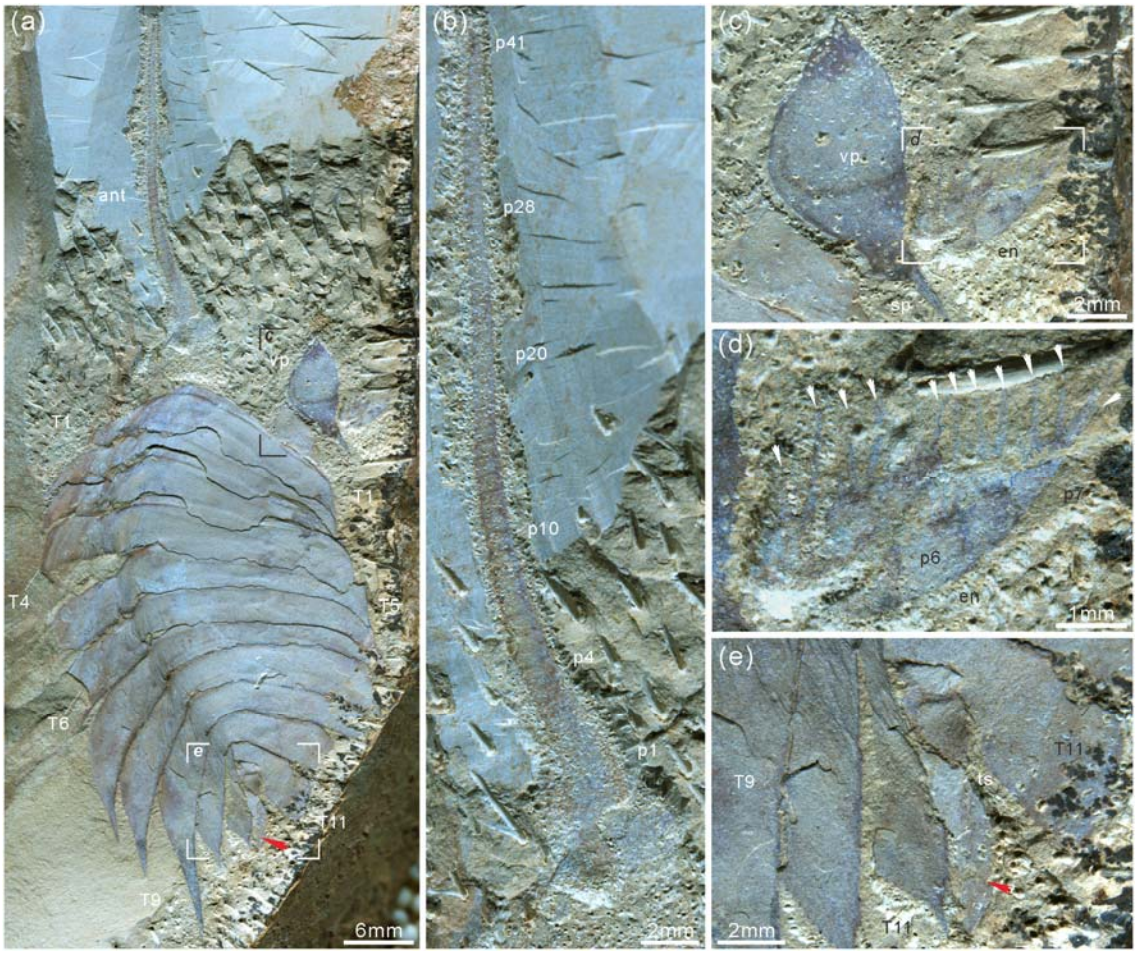

Fig. 3 *Acanthomeridion serratum* from the Cambrian Stage 3 Chengjiang Biota. (a–e) CJHMD 00055, showing the antenna, ventral plate, endopodites with long spines (arrows in d), 11 tergites, and paddle-like structure (red arrow). (a) Overview of whole specimen. (b) Detail of long left antenna. (c) Close-up of ventral plate. (d) Details of long spines (arrows) of right endopodites. (e) Close-up of paddle-like structure (red arrow). Abbreviations same as Fig. 2.

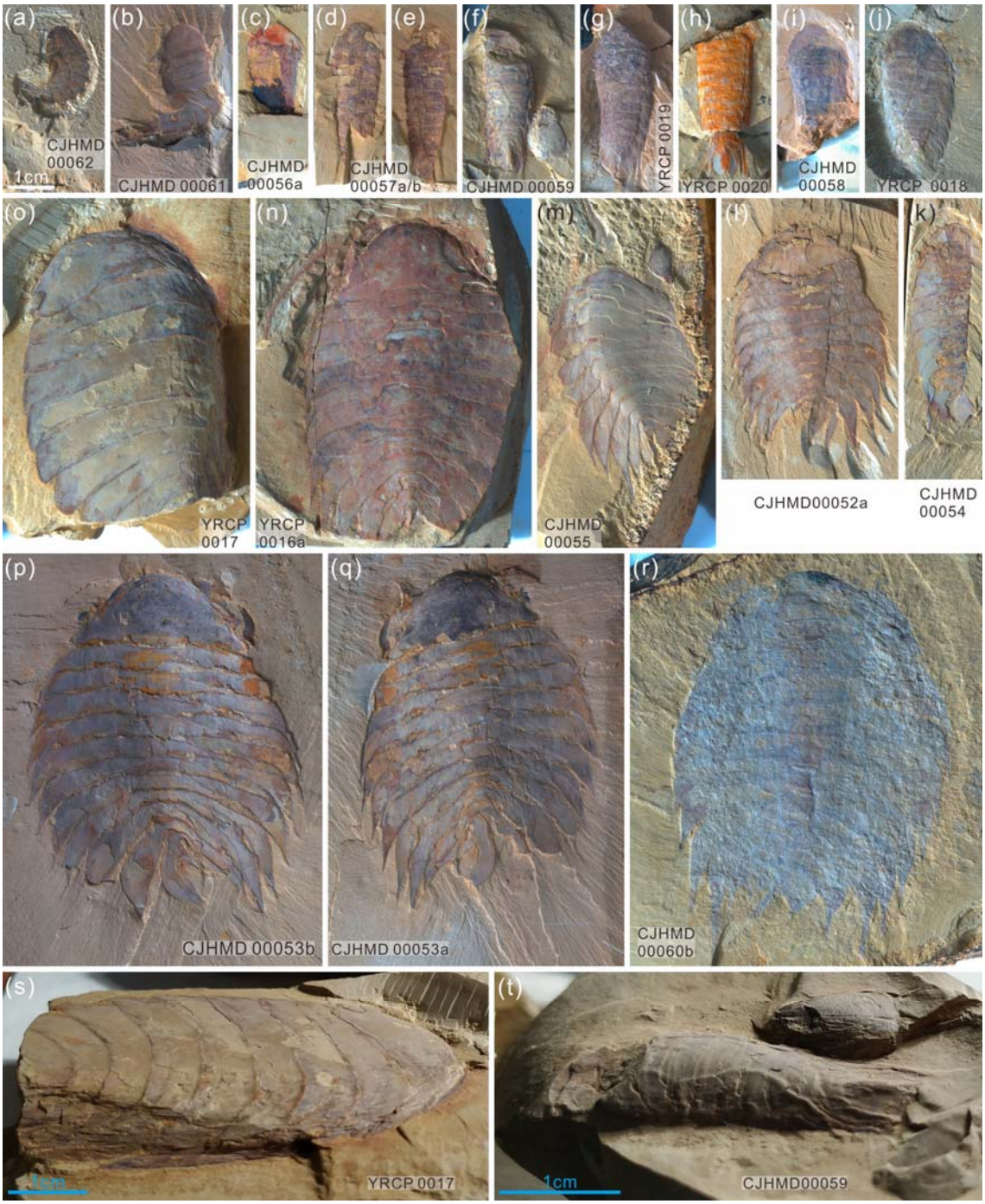

Fig. 4 Ontogenetic series (a–r) of *Acanthomeridion* and their ventrally curling pleurae (s, t). (a–r) Showing the individuals from smallest to largest with same scale bar. (s) Lateral view of (o), note the right curling pleurae and left flat pleurae. (t) Lateral view of (f), showing the left curling pleurae.

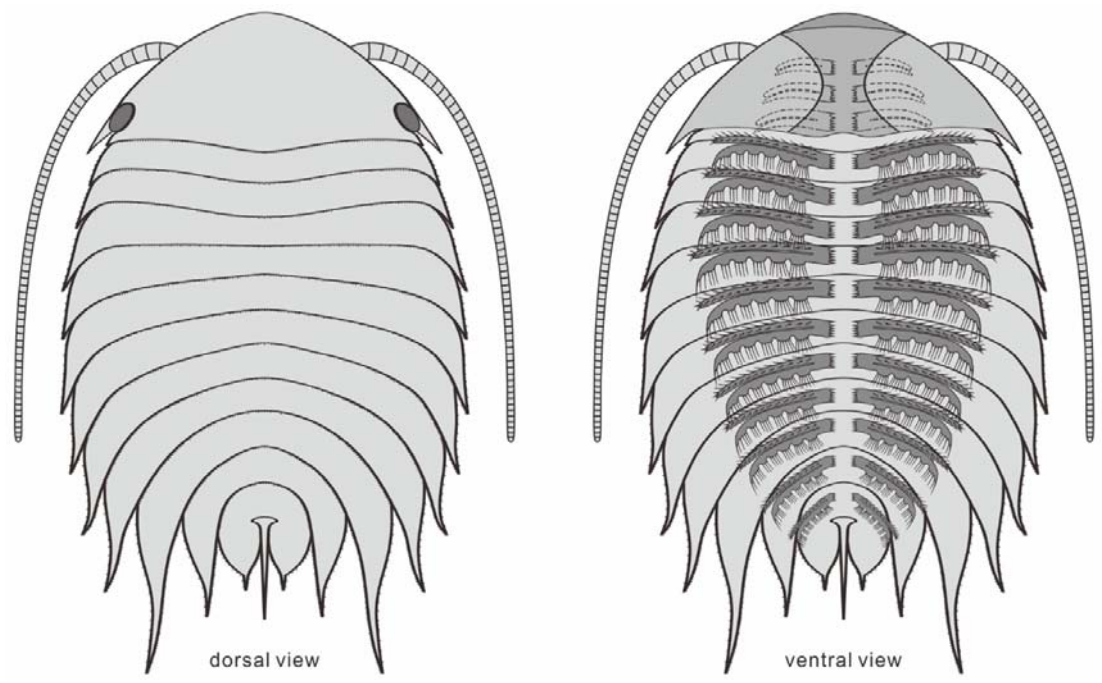

Fig. 5 Artistic reconstruction of *Acanthomeridion serratum*. Only the protopodite of the head appendages have been observed.

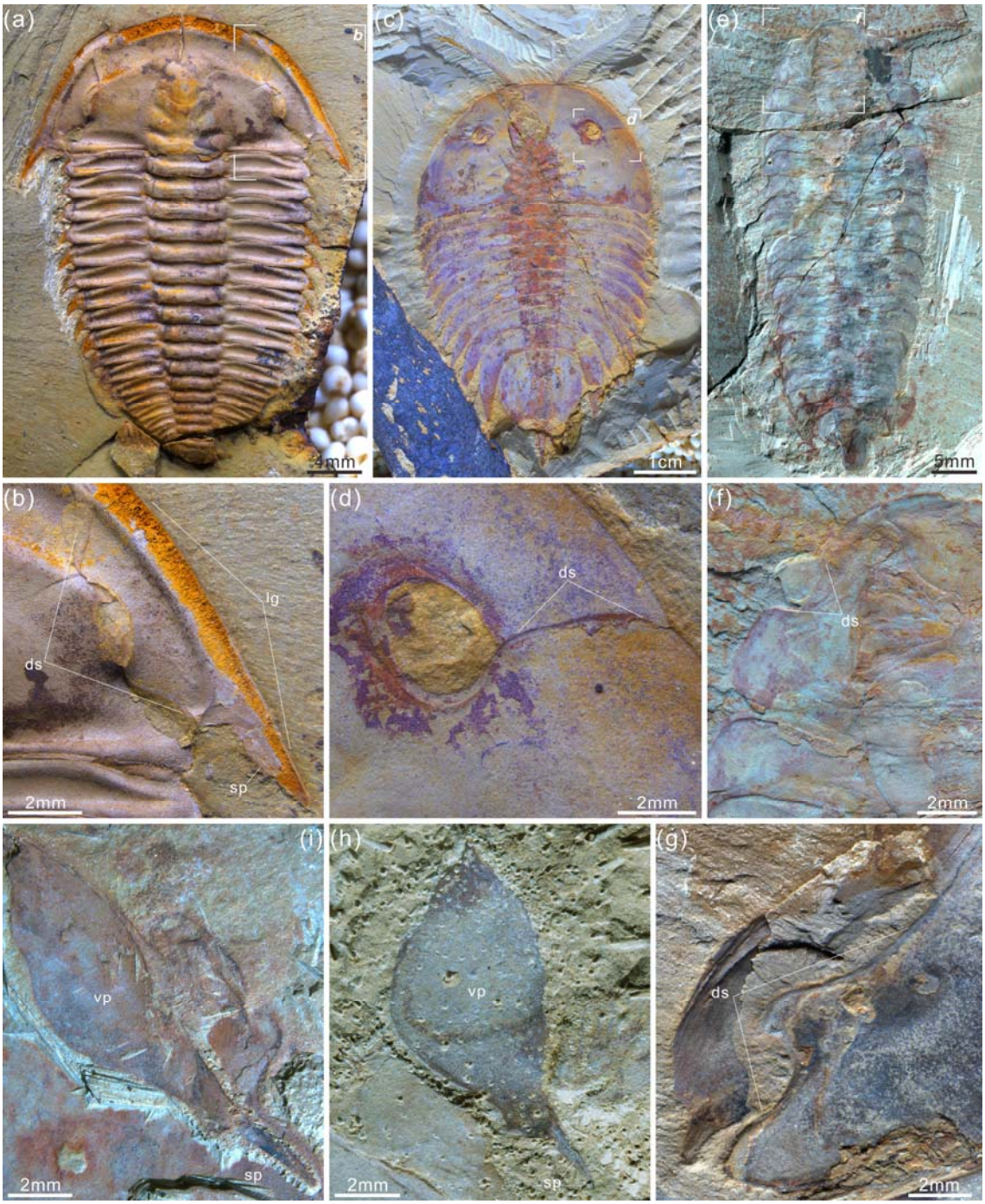

Fig. 6 Four representative artiopodans from early Cambrian with their dorsal sutures, free cheeks and ventral plates. (a, b) The iconic trilobite *Wutingaspis tingi* from Chengjiang Biota, note its free cheeks and dorsal or facial sutures. (c, d) The symbolic xandarellid artiopodan *Xandarella spectaculum* from Chengjiang Biota bearing the distinctive dorsal sutures. (e, f) Holotype of the protosuturan artiopodan *Zhiwenia coronata* from Xiaoshiba Biota developing dorsal sutures. (g) The left dorsal suture of *Acanthomeridion serratum* from Chengjiang Biota, showing the morphological and positional similarities

to that of *W. tingi* (a, b), *X. spectaculum* (c, d), and *Z. coronata* (e, f). (h, i) Right ventral plates of *A. serratum* from Chengjiang Biota bearing a terminal spine, which is similar to free cheek of trilobite like *W. tingi* (a, b).

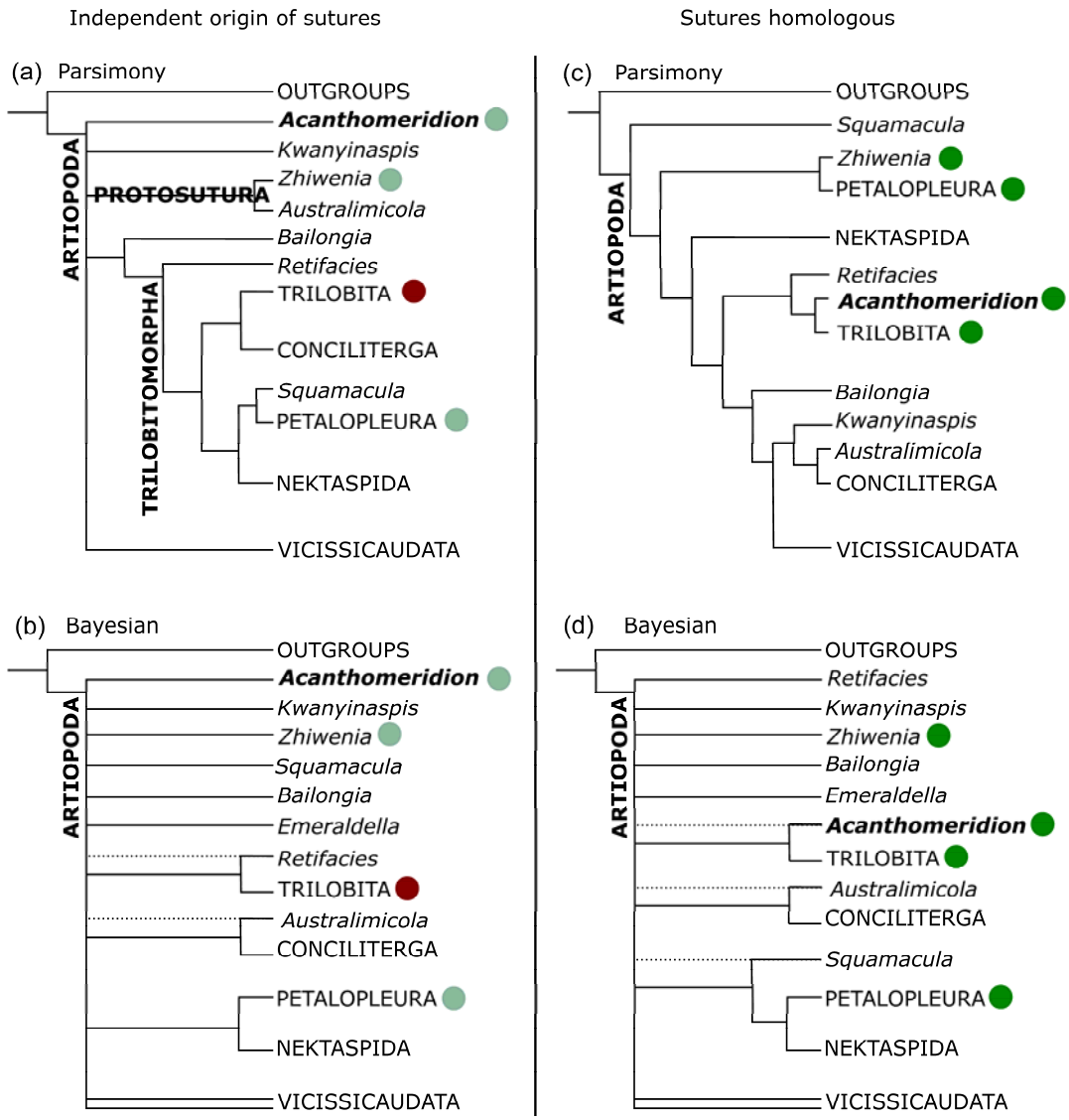

Fig. 7 Simplified results of phylogenetic analyses. (a) Maximum parsimony, a simplified version of Fig. S7a. (b) Bayesian inference, simplified result of Fig. S8a and S9a. (c) Maximum parsimony, a simplified version of Fig. S7b. (d) Bayesian inference, simplified result of Fig. S8b and S9b. Circles indicate presence of cephalic ecdysial sutures. Colors of circles indicate hypothesized homology, as coded in the morphological matrix (either multiple origins – 2 colours – or a single origin – 1 color). Dotted lines indicate the results of minimum assumptions strategy.